Coherence of light scattered from a randomly rough surface

T. A. Leskova, A. A. Maradudin, and J. Munõz-Lopez
Department of Physics and Astronomy and Institute for Surface and Interface Science, University of California, Irvine, California 92697, USA
(Received 24 August 2004; published 14 March 2005)

We study the coherence of *p*-polarized light scattered from a one-dimensional weakly rough random metal surface in contact with vacuum. The mutual coherence function of the single nonzero component of the scattered magnetic field is calculated in planes parallel to, and at increasing distances from, the mean scattering surface in the vacuum region. It is found to be the sum of a contribution that is independent of the distance from the mean surface and a contribution that is a function of this distance and decays to zero over a distance of the order of the wavelength of the incident light. It is also shown that the spatial coherence of the electromagnetic field in the far field in a plane at a fixed distance from the mean surface, as a function of the relative distance along it, mimics the surface height autocorrelation function at short relative distances and oscillates with two periods, $T_1=\lambda$ and $T_2=\lambda/\sin\theta_0$, where θ_0 is the angle of incidence. The former is due to the excitation of lateral waves, while the latter is due to the coherent interference of the multiple scattering processes that lead to the enhanced backscattering effect. In the near field the spatial coherence of the electromagnetic field measured at a fixed distance from the mean surface displays oscillations that are due to the excitation of surface plasmon polaritons. The period of these oscillations equals the wavelength of the surface plasmon polaritons, while the exponential decay of their amplitude is determined by the energy mean free path of the surface plasmon polaritons.

DOI: 10.1103/PhysRevE.71.036606 PACS number(s): 42.25.Kb, 42.25.Fx, 78.68.+m

I. INTRODUCTION

In an early theoretical study of the radiation emitted by a planar quasihomogeneous lambertian source [1], it was predicted that that radiation is not completely spatially incoherent: at a given frequency ω the radiated field correlates over regions whose spatial dimensions are of the order of the wavelength $\lambda=2\pi c/\omega$. This result was obtained by neglecting the contribution of the short-range evanescent waves radiated by the source, and has been successful in describing the coherence properties of thermal emission in the far field. In addition, the coherence properties of the radiation were found to be independent of the distance from the source, when this distance is greater than the wavelength λ.

In the past several years, due to advances in experimental capabilities, and interest in nanoscale phenomena, the coherence properties of optical radiation in the near field from its source have begun to be studied theoretically [2–6]. It is only very recently, however, that these properties have begun to be studied experimentally. In two papers Apostol and Dogariu [7,8] have examined theoretically and experimentally the spatial correlations of optical fields close to a highly scattering randomly inhomogeneous medium as functions of the distance from the surface of the medium. What was measured by these authors were the coherence properties in the near field of light transmitted through highly inhomogeneous media bounded by weakly rough random surfaces. The contribution to these coherence properties from the evanescent field was demonstrated experimentally, and it was shown that they are related to the statistical properties of the surface. In the theoretical studies accompanying the experimental work, the surface of the random medium was considered as being equivalent to a homogeneous, planar, statistically stationary source of optical radiation, characterized by a cross-spectral density function [9] assumed to have a Gaussian form.

In this paper we calculate the spatial correlation of a *p*-polarized optical field of frequency ω scattered from a one-dimensional randomly rough surface of a metal. The plane of incidence is the x_1x_3 plane, and is perpendicular to the generators of the surface. The metal is assumed to be homogeneous, but the surface roughness is treated realistically. We calculate the mutual coherence function $C(x_1,x_3;x_1',x_3|\omega)=\langle H_2(x_1,x_3|\omega)_{sc}H_2(x_1',x_3|\omega)_{sc}^*\rangle$, where $H_2(x_1,x_3|\omega)_{sc}$ is the single nonzero component of the magnetic vector of the scattered light in the vacuum region above the metal surface, and the angle brackets denote an average over the ensemble of realizations of the surface profile function. The calculation of $C(x_1,x_3;x_1',x_3|\omega)$ is carried out through the solution of a Bethe-Salpeter equation [10]. The choice of *p*-polarization for the incident light is due to the fact that the vacuum-metal interface supports a (*p*-polarized) surface plasmon polariton, and the angular dependence of the intensity of the light scattered diffusely displays the enhanced backscattering effect [11]. The effect of each of these properties of the scattering system on the mutual coherence function is examined. We find that $C(x_1,x_3;x_1',x_3|\omega)$ can be written as the sum of a contribution from radiative scattered waves that is independent of x_3, and a contribution from the evanescent scattered waves that is a function of x_3 that decays to zero with increasing x_3 over a distance of a few wavelengths of the incident light.

II. THE SCATTERING SYSTEM

The physical system we consider in this paper consists of vacuum in the region $x_3>\zeta(x_1)$, and a metal, characterized by an isotropic, frequency-dependent, complex dielectric

function $\epsilon(\omega)=\epsilon_1(\omega)+i\epsilon_2(\omega)$, in the region $x_3<\zeta(x_1)$.

The surface profile function $\zeta(x_1)$ is assumed to be a single-valued function of x_1 that is differentiable, and constitutes a stationary, zero-mean Gaussian random process, defined by

$$\langle \zeta(x_1)\zeta(x_1')\rangle = \delta^2 W(|x_1 - x_1'|). \tag{2.1}$$

In Eq. (2.1) and in all that follows the angle brackets denote an average over the ensemble of realizations of $\zeta(x_1)$, and $\delta=\langle \zeta^2(x_1)\rangle^{1/2}$ is the rms height of the surface. The surface height autocorrelation function $W(|x_1|)$ in the present work is assumed to have the Gaussian form

$$W(|x_1|) = \exp(-x_1^2/a^2), \tag{2.2}$$

where the characteristic length a is the transverse correlation length of the surface roughness.

It is convenient to introduce the Fourier integral representation of the surface profile function $\zeta(x_1)$,

$$\zeta(x_1) = \int_{-\infty}^{\infty} \frac{dQ}{2\pi} \hat{\zeta}(Q)\exp(iQx_1). \tag{2.3}$$

The Fourier coefficient $\hat{\zeta}(Q)$ is also a zero-mean Gaussian random process, defined by

$$\langle \hat{\zeta}(Q)\hat{\zeta}(Q')\rangle = 2\pi\delta(Q+Q')\delta^2 g(|Q|), \tag{2.4}$$

where $g(|Q|)$, the power spectrum of the surface roughness is given by

$$g(|Q|) = \int_{-\infty}^{\infty} dx_1 W(|x_1|)\exp(-iQx_1) \tag{2.5a}$$

$$= \sqrt{\pi} a \exp(-a^2Q^2/4). \tag{2.5b}$$

III. THE MUTUAL COHERENCE FUNCTION

The surface $x_3=\zeta(x_1)$ is illuminated from the vacuum by a p-polarized plane wave of frequency ω, whose plane of incidence is the x_1x_3 plane. The single nonzero component of the magnetic vector in the vacuum region $x_3>\zeta(x_1)_{\max}$ that satisfies the boundary conditions at infinity is the sum of an incoming incident plane wave and of outgoing scattered waves,

$$H_2(x_1,x_3|\omega) = \exp[ikx_1 - i\alpha_0(k)x_3] + \int_{-\infty}^{\infty} \frac{dq}{2\pi} R(q|k) \times \exp[iqx_1 + i\alpha_0(q)x_3], \tag{3.1}$$

where $\alpha_0(q)=[(\omega/c)^2-q^2]^{1/2}$, with $\mathrm{Re}\,\alpha_0(q)>0$, $\mathrm{Im}\,\alpha_0(q)>0$. A time dependence of the field of the form $\exp(-i\omega t)$ has been assumed, but has not been indicated explicitly.

We are concerned here with the evaluation of the correlation function (the mutual coherence function)

$$C(x_1,x_3;x_1',x_3'|\omega) = \langle H_2(x_1,x_3|\omega)_{\mathrm{sc}} H_2(x_1',x_3'|\omega)^*_{\mathrm{sc}}\rangle, \tag{3.2}$$

where $x_3>\zeta(x_1)$ and $x_3'>\zeta(x_1')$, and $H_2(x_1,x_3|\omega)_{\mathrm{sc}}$, the scattered field, is given by the second term on the right-hand side of Eq. (3.1). The elements of the mutual coherence tensor $\langle E_i(x_1,x_3|\omega)_{\mathrm{sc}} E_j(x_1',x_3'|\omega)^*_{\mathrm{sc}}\rangle$ where $i,j=1,3$, are then obtained from $C(x_1,x_3;x_1',x_3|\omega)$ according to

$$\langle E_1(x_1,x_3|\omega)_{\mathrm{sc}} E_1(x_1',x_3'|\omega)^*_{\mathrm{sc}}\rangle = \left(\frac{c}{\omega}\right)^2 \frac{\partial^2}{\partial x_3\,\partial x_3'} \times C(x_1,x_3;x_1';x_3'|\omega), \tag{3.3a}$$

$$\langle E_1(x_1,x_3|\omega)_{\mathrm{sc}} E_3(x_1',x_3'|\omega)^*_{\mathrm{sc}}\rangle = -\left(\frac{c}{\omega}\right)^2 \frac{\partial^2}{\partial x_3\,\partial x_1'} \times C(x_1,x_3;x_1';x_3'|\omega), \tag{3.3b}$$

$$\langle E_3(x_1,x_3|\omega)_{\mathrm{sc}} E_1(x_1',x_3'|\omega)^*_{\mathrm{sc}}\rangle = -\left(\frac{c}{\omega}\right)^2 \frac{\partial^2}{\partial x_1\,\partial x_3'} \times C(x_1,x_3;x_1',x_3'|\omega), \tag{3.3c}$$

$$\langle E_3(x_1,x_3|\omega)_{\mathrm{sc}} E_3(x_1',x_3'|\omega)^*_{\mathrm{sc}}\rangle = \left(\frac{c}{\omega}\right)^2 \frac{\partial^2}{\partial x_1\,\partial x_1'} \times C(x_1,x_3;x_1';x_3'|\omega). \tag{3.3d}$$

On combining Eqs. (3.1) and (3.2) we obtain the result

$$C(x_1,x_3;x_1',x_3'|\omega) = \int_{-\infty}^{\infty} \frac{dq}{2\pi} \int_{-\infty}^{\infty} \frac{dq'}{2\pi} \times \exp\{i(qx_1 - q'x_1') + i[\alpha_0(q)x_3 - \alpha_0^*(q')x_3']\}\langle R(q|k)R^*(q'|k)\rangle. \tag{3.4}$$

In what follows we will focus our attention on the correlation function $\langle R(q|k)R^*(q'|k)\rangle$.

In what follows we assume that the surface is weakly rough so that the Rayleigh hypothesis [12] is applicable. This means that the expression (3.1) for the magnetic field in the vacuum region which, strictly speaking, is valid only for $x_3>\zeta(x_1)_{\max}$, can be used in satisfying the boundary conditions at the surface $x_3=\zeta(x_1)$ itself. Although rigorous limits of validity of the Rayleigh hypothesis for a one-dimensional randomly rough surface are not known, by analogy with the known limits of its validity for one-dimensional periodically corrugated surfaces [13] it is believed that it is valid when the inequality $|d\zeta(x_1)/dx_1| \ll 1$ holds In this case the scattering amplitude $R(q|k)$ satisfies the reduced Rayleigh equation [14]

$$\int_{-\infty}^{\infty} \frac{dq}{2\pi} N^{(+)}(p|q)R(q|k) = -N^{(-)}(p|k), \tag{3.5}$$

where

$$N^{(+)}(p|q) = \frac{I(\alpha(p) - \alpha_0(q)|p-q)}{\alpha(p) - \alpha_0(q)}[pq + \alpha(p)\alpha_0(q)], \tag{3.6a}$$

$$N^{(-)}(p|k) = \frac{I(\alpha(p) + \alpha_0(k)|p-k)}{\alpha(p) + \alpha_0(k)}[pk - \alpha(p)\alpha_0(k)], \tag{3.6b}$$

and $\alpha(k) = [\epsilon(\omega)(\omega/c)^2 - q^2]^{1/2}$, with $\mathrm{Re}\,\alpha(q) > 0$, $\mathrm{Im}\,\alpha(q) > 0$. The function $I(\gamma|Q)$ appearing in Eqs. (3.6) is defined by

$$I(\gamma|Q) = \int_{-\infty}^{\infty} dx_1 \exp(-iQx_1)\exp[-i\gamma\zeta(x_1)]. \tag{3.7}$$

We seek the solution of Eq. (3.5) in the form [15]

$$R(q|k) = 2\pi\delta(q-k)R_0(k) - 2iG_0(q)T(q|k)G_0(k)\alpha_0(k), \tag{3.8}$$

where

$$R_0(k) = \frac{\epsilon(\omega)\alpha_0(k) - \alpha(k)}{\epsilon(\omega)\alpha_0(k) + \alpha(k)} \tag{3.9}$$

is the Fresnel coefficient for the reflection of *p*-polarized light from a planar vacuum-metal interface, and

$$G_0(k) = \frac{i\epsilon(\omega)}{\epsilon(\omega)\alpha_0(k) + \alpha(k)} \tag{3.10}$$

is the Green's function for a surface plasmon polariton at a planar, vacuum-metal interface. The transition matrix $T(q|k)$ is postulated to satisfy the equation

$$T(q|k) = V(q|k) + \int_{-\infty}^{\infty} \frac{dp}{2\pi} T(q|p)G_0(p)V(p|k). \tag{3.11}$$

Equations (3.5), (3.8), and (3.11) define the scattering potential $V(q|k)$ that appears in Eq. (3.11). From these equations we find that this potential is the solution of the equation [14]

$$\int_{-\infty}^{\infty} \frac{dq}{2\pi}[N^{(+)}(p|q) - N^{(-)}(p|q)]\frac{V(q|k)}{2i\alpha_0(q)} = \{N^{(+)}(p|k)[\epsilon(\omega)\alpha_0(k) - \alpha(k)] + N^{(-)}(p|k)[\epsilon(\omega)\alpha_0(k) + \alpha(k)]\}\frac{1}{2\epsilon(\omega)\alpha_0(k)}. \tag{3.12}$$

We now introduce the Green's function $G(q|k)$ for surface plasmon polaritons on the randomly rough surface, which is defined by

$$G(q|k) = 2\pi\delta(q-k)G_0(k) + G_0(q)T(q|k)G_0(k). \tag{3.13}$$

By combining Eqs. (3.8) and (3.13), and using the definitions (3.9) and (3.10), we obtain the useful relation

$$R(q|k) = -2\pi\delta(q-k) - 2iG(q|k)\alpha_0(k). \tag{3.14}$$

From Eq. (3.14) we immediately obtain the result

$$\langle R(q|k)R^*(q'|k)\rangle = \langle R(q|k)\rangle\langle R^*(q'|k)\rangle + 4[\langle G(q|k)G^*(q'|k)\rangle - \langle G(q|k)\rangle \times \langle G^*(q'|k)\rangle]\alpha_0^2(k). \tag{3.15}$$

We will evaluate the two contributions on the right-hand side of Eq. (3.15) in turn.

From Eq. (3.14) we find that

$$\langle R(q|k)\rangle = 2\pi\delta(q-k) - 2i\langle G(q|k)\rangle\alpha_0(k). \tag{3.16}$$

Due to the stationarity of the surface profile function $\zeta(x_1)$ the averaged Green's function $\langle G(q|k)\rangle$ is diagonal in q and k,

$$\langle G(q|k)\rangle = 2\pi\delta(q-k)G(k). \tag{3.17}$$

The Green's function $G(k)$ is related to the unperturbed Green's function $G_0(k)$ by [10]

$$G(k) = \frac{1}{G_0(k)^{-1} - M(k)} = \frac{i\epsilon(\omega)}{\epsilon(\omega)\alpha_0(k) + \alpha(k) - i\epsilon(\omega)M(k)}, \tag{3.18}$$

where $M(k)$ is a proper self-energy that is obtained from the pair of equations [10]

$$\langle M(q|k)\rangle = 2\pi\delta(q-k)M(k),$$

$$M(q|k) = V(q|k) + \int_{-\infty}^{\infty}\frac{dp}{2\pi}\int_{-\infty}^{\infty}\frac{dr}{2\pi}M(q|p)\langle G(p|r)\rangle \times [V(r|k) - \langle M(r|k)\rangle]. \tag{3.19}$$

When we combine Eqs. (3.16)–(3.18) and use the definition (3.10), we find that

$$\langle R(q|k)\rangle = 2\pi\delta(q-k)R(k), \tag{3.20a}$$

where

$$R(k) = \frac{\epsilon(\omega)\alpha_0(k) - \alpha(k) + i\epsilon(\omega)M(k)}{\epsilon(\omega)\alpha_0(k) + \alpha(k) - i\epsilon(\omega)M(k)}. \tag{3.20b}$$

It follows from Eqs. (3.4), (3.15), and (3.20a) that

$$C(x_1,x_3;x_1',x_3'\omega) = |R(k)|^2\exp[ik(x_1 - x_1') + i\alpha_0(k)(x_3 - x_3')] + 4\alpha_0^2(k)\int_{-\infty}^{\infty}\frac{dq}{2\pi}\int_{-\infty}^{\infty}\frac{dq'}{2\pi}\exp\{i(qx_1 - q'x_1') + i[\alpha_0(q)x_3 - \alpha_0^*(q')x_3']\} \times [\langle G(q|k)G^*(q'|k)\rangle - \langle G(q|k)\rangle \times \langle G^*(q'|k)\rangle]. \tag{3.21}$$

IV. THE BETHE-SALPETER EQUATION

Equation (3.21) is convenient for the determination of $C(x_1,x_3;x_1',x_3'|\omega)$ because $\langle G(q|k)G^*(q'|k)\rangle - \langle G(q|k)\rangle$

$\times\langle G^*(q'|k)\rangle$ can be calculated from the solution of the Bethe-Salpeter equation [10],

$$\langle G(q|k)G^*(q'|k')\rangle = \langle G(q|k)\rangle\langle G^*(q'|k')\rangle + \int_{-\infty}^{\infty}\frac{dr}{2\pi}\int_{-\infty}^{\infty}\frac{dr'}{2\pi}\int_{-\infty}^{\infty}\frac{ds}{2\pi}\int_{-\infty}^{\infty}\frac{ds'}{2\pi} \times\langle G(q|r)\rangle\langle G^*(q'|r')\rangle\langle\Gamma(r,r'|s,s')\rangle \times\langle G(s|k)G^*(s'|k')\rangle, \tag{4.1}$$

where $\langle\Gamma(r,r'|s,s')\rangle$ is the irreducible vertex function. If we make use of Eq. (3.17), Eq. (4.1) becomes

$$\langle G(q|k)G^*(q'|k')\rangle = 2\pi\delta(q-k)2\pi\delta(q'-k')G(q)G^*(q') + G(q)G^*(q')\int_{-\infty}^{\infty}\frac{ds}{2\pi}\int_{-\infty}^{\infty}\frac{ds'}{2\pi} \times\langle\Gamma(q,q'|s,s')\rangle\langle G(s|k)G^*(s'|k')\rangle. \tag{4.2}$$

We now set $k'=k$ and obtain

$$\langle G(q|k)G^*(q'|k)\rangle = 2\pi\delta(q-q')2\pi\delta(q-k)|G(k)|^2 + G(q)G^*(q')\int_{-\infty}^{\infty}\frac{ds}{2\pi}\int_{-\infty}^{\infty}\frac{ds'}{2\pi} \times\langle\Gamma(q,q'|s,s')\rangle\langle G(s|k)G^*(s'|k)\rangle. \tag{4.3}$$

To solve Eq. (4.3) we write

$$\langle G(q|k)G^*(q'|k)\rangle = 2\pi\delta(q-q')\Phi(q|k), \tag{4.4}$$

a result that follows from the stationarity of the surface profile function. The stationarity of the surface profile function has the further consequence that $\langle\Gamma(q,q'|s,s)\rangle$ is diagonal in q and q',

$$\langle\Gamma(q,q'|s,s)\rangle = 2\pi\delta(q-q')U(q|s). \tag{4.5}$$

The equation satisfied by $\Phi(q|k)$ therefore becomes

$$\Phi(q|k) = 2\pi\delta(q-k)|G(k)|^2 + |G(q)|^2\int_{-\infty}^{\infty}\frac{ds}{2\pi}U(q|s)\Phi(s|k). \tag{4.6}$$

The solution of Eq. (4.6) can be written formally as

$$\Phi(q|k) = 2\pi\delta(q-k)|G(k)|^2 + |G(q)|^2\hat{R}(q|k)|G(k)|^2, \tag{4.7}$$

where $\hat{R}(q|k)$ is the reducible vertex function. It is related to the irreducible vertex function $U(q|k)$ by

$$\hat{R}(q|k) = U(q|k) + \int_{-\infty}^{\infty}\frac{ds}{2\pi}U(q|s)|G(s)|^2\hat{R}(s|k). \tag{4.8}$$

If we multiply both sides of Eq. (4.7) by $2\pi\delta(q-q')$, then in view of Eq. (4.4) we obtain

$$\langle G(q|k)G^*(q'|k)\rangle - \langle G(q|k)\rangle\langle G^*(q'|k)\rangle = 2\pi\delta(q-q')|G(q)|^2\hat{R}(q|k)|G(k)|^2. \tag{4.9}$$

It follows from Eqs. (3.21) and (4.9) that

$$C(x_1,x_3;x_1',x_3'|\omega) = |R(k)|^2\exp[ik(x_1-x_1') + i\alpha_0(k)(x_3-x_3')] + 4\alpha_0^2(k)\int_{-\infty}^{\infty}\frac{dq}{2\pi}\exp\{iq(x_1-x_1') + i[\alpha_0(q)x_3 - \alpha_0^*(q)x_3']\} \times|G(q)|^2\hat{R}(q|k)|G(k)|^2. \tag{4.10}$$

This result is exact within the limits of validity of the Rayleigh hypothesis [12]. We now turn to a determination of $\hat{R}(q|k)$.

We approximate the irreducible vertex function $U(q|k)$ by the sum of the contributions from all maximally-crossed diagrams, because they describe the phase coherent multiple-scattering processes that give rise to enhanced backscattering. In calculating these contributions we make the small roughness approximation [14], which consists of approximating the scattering potential $V(q|k)$ by the solution of Eq. (3.12) that is of first order in the surface profile function $\zeta(x_1)$,

$$V(q|k) \cong u(q|k)\hat{\zeta}(q-k), \tag{4.11}$$

where

$$u(q|k) = \frac{\epsilon(\omega)-1}{\epsilon^2(\omega)}[\epsilon(\omega)qk - \alpha(q)\alpha(k)] = u(k|q) = u(-q|-k) = u(-k|-q). \tag{4.12}$$

The results we obtain are therefore limited to weakly rough surfaces.

We also make the (inessential) approximation of neglecting the imaginary part of $\epsilon(\omega)$ in evaluating $u(q|k)$. This has the consequence that $u(q|k)$ is real in the frequency range in which the real part of $\epsilon(\omega)$ is negative, which contains the frequency range in which surface plasmon polaritons can exist.

In the small roughness approximation, Eq. (4.11), the proper self-energy $M(k)$ is given by

$$M(k) = \delta^2\int_{-\infty}^{\infty}\frac{dp}{2\pi}[u(k|p)]^2G_0(p)g(|p-k|). \tag{4.13}$$

In calculating $U(q|k)$ we also use the pole approximation for the averaged Green's function $G(s)$ [11]

$$G(s) \simeq \frac{C(\omega)}{s - k_{sp}(\omega) - i\Delta(\omega)} - \frac{C(\omega)}{s + k_{sp}(\omega) + i\Delta(\omega)}, \tag{4.14}$$

where

$$\Delta(\omega) = \Delta_{\epsilon}(\omega) + \Delta_{\mathrm{sp}}(\omega), \tag{4.15}$$

with

$$\Delta_{\epsilon}(\omega) = \frac{1}{2}\frac{\omega}{c}\frac{\epsilon_2(\omega)}{|\epsilon_1(\omega)|^{1/2}(|\epsilon_1(\omega)|-1)^{3/2}}, \tag{4.16}$$

$$\Delta_{\mathrm{sp}}(\omega) = 2C^2(\omega)\left(\frac{\omega}{c}\right)^4\left[\frac{\epsilon_1^2(\omega)}{|\epsilon_1(\omega)|-1}\right]^2\delta^2 g(2k_{\mathrm{sp}}(\omega)), \tag{4.17}$$

$$C(\omega) = \frac{|\epsilon_1(\omega)|^{3/2}}{\epsilon_1^2(\omega)-1}, \tag{4.18}$$

$$k_{\mathrm{sp}}(\omega) = \frac{\omega}{c}\left[\frac{|\epsilon_1(\omega)|}{|\epsilon_1(\omega)|-1}\right]^{1/2}. \tag{4.19}$$

Here $\Delta_{\epsilon}(\omega)$ is the amplitude decay rate of the surface plasmon polariton of frequency ω supported by a planar vacuum-metal interface, whose wave number is $k_{\mathrm{sp}}(\omega)$, and $\Delta_{\mathrm{sp}}(\omega)$ is the amplitude decay rate of the suface plasmon polariton due to its roughness-induced scattering into other surface plasmon polaritons. The result is [16]

$$U(q|k) = X(q|k) + \frac{A(q|k)}{(q+k)^2+4\Gamma^2}, \tag{4.20}$$

where

$$\begin{aligned} A(q|k) = {} & 2C^2(\omega)\Delta(\omega)[X(q|k_{\mathrm{sp}})X(k_{\mathrm{sp}}|k) + X(q|-k_{\mathrm{sp}}) \\ & \times X(-k_{\mathrm{sp}}|k)] + 2C^2(\omega)\Delta_{\mathrm{sp}}(\omega)[X(q|k_{\mathrm{sp}})X(-k_{\mathrm{sp}}|k) \\ & + X(q|-k_{\mathrm{sp}})X(k_{\mathrm{sp}}|k)], \end{aligned} \tag{4.21}$$

$$X(q|k) = [u(q|k)]^2\delta^2 g(|q-k|), \tag{4.22}$$

$$\Gamma = [\Delta_{\epsilon}(\Delta_{\epsilon}+2\Delta_{\mathrm{sp}})]^{1/2}. \tag{4.23}$$

When the result given by Eq. (4.20) is substituted into Eq. (4.8) the resulting equation,

$$\begin{aligned} \hat{R}(q|k) = {} & X(q|k) + \frac{A(q|k)}{(q+k)^2+4\Gamma^2} + \int_{-\infty}^{\infty}\frac{ds}{2\pi}\left[X(q|s)\right. \\ & \left. + \frac{A(q|s)}{(q+s)^2+4\Gamma^2}\right]|G(s)|^2\hat{R}(s|k), \end{aligned} \tag{4.24}$$

is solved by iteration. However, in each of the resulting integral terms only the contribution associated with $X(q|k)$ is kept, and all terms that contain $A(q|k)/[(q+k)^2+4\Gamma^2]$ are omitted. The sum of the integral terms obtained in this way is just the sum of the contributions from all ladder diagrams of two or more rungs. The reason for this approximation is that the contribution to $\hat{R}(q|k)$ from the ladder diagrams is equal to the contribution from $A(q|k)/[(q+k)^2+4\Gamma^2]$, the second term on the right hand side of Eq. (4.24), when $q=-k$, i.e., in the backscattering direction, while the integral terms containing $A(q|k)/[(q+k)^2+4\Gamma^2]$ are small in comparison [17]. In this way we obtain the result that

$$\hat{R}(q|k) = X(q|k) + \frac{A(q|k)}{4\Gamma^2} + \frac{A(q|k)}{(q+k)^2+4\Gamma^2}. \tag{4.25}$$

The first term on the right-hand side of Eq. (4.25) is the contribution to $\hat{R}(q|k)$ from single-scattering processes; the second term is the contribution from all ladder diagrams of two or more rungs; and the third term is the contribution from the maximally-crossed diagrams. We see that the second and third terms are equal when $q=-k$. This means that the height of the peak in $\hat{R}(q|k)$ at $q=-k$ is twice the height of the background at its position when the contribution from the single-scattering processes is subtracted off. It is the peak in $\hat{R}(q|k)$ arising from the third term on the right hand side of Eq. (4.25) that describes enhanced backscattering. This conclusion follows from the result that the contribution to the mean differential reflection coefficient from the light that has been scattered incoherently, calculated on the basis of the approximations used in obtaining $\hat{R}(q|k)$ is given by [17]

$$\begin{aligned} \left\langle\frac{\partial R_p}{\partial\theta_s}\right\rangle_{\mathrm{incoh}} = {} & \frac{2}{\pi}\left(\frac{\omega}{c}\right)^3\cos^2\theta_s\cos\theta_0|G(q)|^2\left[X(q|k) + \frac{A(q|k)}{4\Gamma^2}\right. \\ & \left. + \frac{A(q|k)}{(q+k)^2+4\Gamma^2}\right]|G(k)|^2, \end{aligned} \tag{4.26}$$

where the wave numbers k and q are to be expressed in terms of the angles of incidence and scattering θ_0 and θ_s, measured counterclockwise and clockwise from the positive x_3 axis, respectively, through $k=(\omega/c)\sin\theta_0$ and $q=(\omega/c)\sin\theta_s$.

When the result given by Eq. (4.25) is substituted into Eq. (4.10) and x_3' is set equal to x_3, the correlation function $C(x_1,x_3;x_1',x_3|\omega)$ takes the form

$$\begin{aligned} C(x_1,x_3;x_1',x_3|\omega) = {} & |R(k)|^2\exp[ik(x_1-x_1')] + C(x_1;x_1'|\omega)_{\mathrm{hom}} \\ & + C(x_1,x_3;x_1',x_3|\omega)_{\mathrm{ev}}, \end{aligned} \tag{4.27}$$

where

$$\begin{aligned} C(x_1;x_1'|\omega)_{\mathrm{hom}} = {} & 4\alpha_0^2(k)\int_{|q|<\omega/c}\frac{dq}{2\pi}|G(q)|^2\left[X(q|k) + \frac{A(q|k)}{4\Gamma^2}\right. \\ & \left. + \frac{A(q|k)}{(q+k)^2+4\Gamma^2}\right]|G(k)|^2\exp[iq(x_1-x_1')], \end{aligned} \tag{4.28}$$

$$\begin{aligned} C(x_1,x_3;x_1',x_3|\omega)_{\mathrm{ev}} = {} & 4\alpha_0^2(k)\int_{|q|>(\omega/c)}\frac{dq}{2\pi}|G(q)|^2\left[X(q|k)\right. \\ & \left. + \frac{A(q|k)}{4\Gamma^2} + \frac{A(q|k)}{(q+k)^2+4\Gamma^2}\right] \\ & \times|G(k)|^2\exp[iq(x_1-x_1')] \\ & \times\exp[-2\beta_0(q)x_3], \end{aligned} \tag{4.29}$$

where

$$\beta_0(q) = [q^2 - (\omega/c)^2]^{1/2} \quad \mathrm{Re}\,\beta_0(q) > 0, \quad \mathrm{Im}\,\beta_0(q) < 0. \tag{4.30}$$

The contribution $|R(k)|^2 \exp[ik(x_1 - x_1')] + C(x_1; x_1'|\omega)_{\mathrm{hom}}$ is independent of x_3. The contribution $C(x_1, x_3; x_1', x_3|\omega)_{\mathrm{ev}}$ is a function of x_3 that decays to zero with increasing x_3.

Finally, we emphasize that although the pole approximation (4.14) for $G(s)$ was used in calculating the irreducible vertex function $U(q|k)$, it is the result for $G(q)$ obtained by combining Eqs. (3.18) and (4.13) that is used in evaluating the integrals over q in Eqs. (4.27) and (4.28). Therefore, the integrands in Eqs. (4.27) and (4.28) have branch points at $q = \pm(\omega/c)$ arising from the presence of $\alpha_0(q)$ in the expression (3.18) for $G(q)$. In addition, $G(q)$ has simple poles at $q = \pm[k_{\mathrm{sp}}(\omega) + i\Delta(\omega)]$, i.e., at the wave numbers of the surface plasmon polaritons on the randomly rough surface. Finally, the integrands in Eqs. (4.27) and (4.28) have poles at $q = -k \pm i2\Gamma$, which are associated with the existence of a peak in the retroreflection direction in the angular dependence of the intensity of the light scattered incoherently. All of these singularities manifest themselves in the dependencies of $C(x_1; x_1'|\omega)_{\mathrm{hom}}$ and $C(x_1, x_3; x_1', x_3|\omega)_{\mathrm{ev}}$ on x_1 and x_3.

V. RESULTS

We have carried out calculations of $C(x_1, x_3; x_1', x_3|\omega)$ for three different one-dimensional randomly rough silver surfaces. All three are characterized by an rms height $\delta = 5$ nm. One of them (surface *A*) is characterized by a transverse correlation length $a = 100$ nm; the second (surface *B*) is characterized by a transverse correlation length $a = 200$ nm; while the third (surface *C*) is characterized by a transverse correlation length $a = 400$ nm. The wavelength of the incident, *p*-polarized light is $\lambda = 457.9$ nm, and the dielectric function of silver at this wavelength is $\epsilon(\omega) = 7.5 + i0.24$ [18].

The three surfaces differ significantly in their scattering properties. Surface *A*, when illuminated at normal incidence, produces a well-defined peak in the retroreflection direction in the contribution to the mean differential reflection coefficient from the light that has been scattered incoherently (diffusely), $\langle \partial R/\partial\theta_s \rangle_{\mathrm{incoh}}$ [Fig. 1(a)]. This is the well known enhanced backscattering effect. This peak is weaker but still visible in the angular dependence of $\langle \partial R/\partial\theta_s \rangle_{\mathrm{incoh}}$ when surface *B* is illuminated at normal incidence [Fig. 1(b)]. Surface *C*, when illuminated at normal incidence, displays no such peak in $\langle \partial R_p/\partial\theta_s \rangle_{\mathrm{incoh}}$ [Fig. 1(c)]. [In fact, if the vertical scale in Fig. 1(c) were magnified significantly, a peak in the retroreflection direction would be observed, but it is too weak to be seen on the scale of Fig. 1(c).] What is displayed in Fig. 1(c) is essentially a scaled version of the power spectrum of the surface roughness. These differences in the scattering behaviors of the three surfaces will manifest themselves in the results of the calculations of $C(x_1, x_3; x_1', x_3|\omega)$ for each of them.

In Figs. 2(a)–2(d) plots of the correlation function $C(x_1, x_3; x_1', x_3|\omega) = |R(k)|^2 \exp[ik(x_1 - x_1')] + C(x_1; x_1'|\omega)_{\mathrm{hom}} + C(x_1, x_3; x_1', x_3|\omega)_{\mathrm{ev}}$ as a function of $(x_1 - x_1')/\lambda$ and x_3/λ are presented for the case when *p*-polarized light of wavelength λ is incident normally on (a) surface *A* and on (b) surface *C*; and (c) and (d) when the light is incident at an angle $\theta_0 = 20°$ on surface *A*.

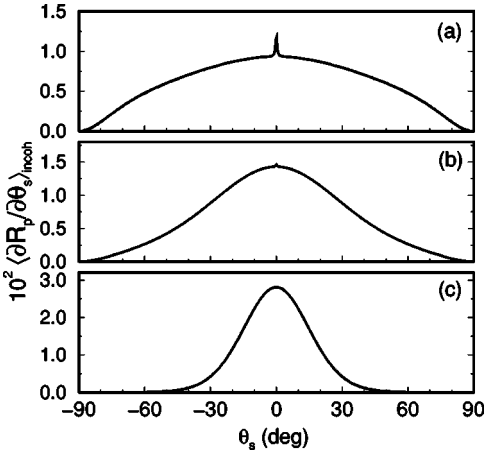

FIG. 1. The contribution to the mean differential reflection coefficient from the light scattered incoherently when *p*-polarized light is incident normally on a one-dimensional randomly rough silver surface. (a) Surface *A*; (b) surface *B*; (c) surface *C*.

The correlation functions shown in Figs. 2(a) and 2(b) decrease with increasing x_3 over a distance of the order of λ to a constant that is the value of $|R(k)|^2 + C(x_1; x_1|\omega)_{\mathrm{hom}}$ for $x_1 - x_1' = 0$. The only contribution to $C(x_1, x_3; x_1, x_3|\omega)$ that depends on the distance from the mean surface, $C(x_1, x_3; x_1, x_3|\omega)_{\mathrm{ev}}$, at $x_3 = 0$ can reach quite large values due to the strong enchancement of the surface polariton field at the surface. For surface *A* [Figs. 2(a), 2(c), and 2(d)] it is of the same order of magnitude as $|R(k)|^2 + C(x_1; x_1|\omega)_{\mathrm{hom}}$ (it is approximately a factor of two larger), and is three orders of magnitude smaller for surface *C* [Fig. 1(a)] than it is for surface *A*. This is because the roughness induced excitation of surface plasmon polaritons is considerably weaker for this surface. Although on the scale of this figure it appears as if $|R(k)|^2 + C(x_1; x_1|\omega)_{\mathrm{hom}}$ has the same value for surface *C* as it does for surface *A*, in fact it differs slightly due to different values of $|R(0)|^2$ (0.95293 for surface *A* and 0.96067 for surface *C*), and $C(x_1; x_1'|\omega)_{\mathrm{hom}}$ (0.02775 for surface *A* and 0.01998 for surface *C* at $x_1 - x_1' = 0$). When light is incident normally on a surface, $k = 0$, the function $X(q|k)$, given by Eqs. (4.22) and (4.23) is an even function of q, and the single scattering contributions to the correlation functions $C(x_1; x_1'|\omega)_{\mathrm{hom}}$ and $C(x_1, x_3; x_1', x_3|\omega)_{\mathrm{ev}}$ are real, while their imaginary parts are determined solely by the contributions from the multiple scattering processes and are negligibly small. However, this is not the case at oblique incidence, which is clearly illustrated in Fig. 2(d).

The dependence of the correlation functions $C(x_1, x_3; x_1', x_3|\omega)$ on $(x_1 - x_1')$ shown in Figs. 2(a)–2(d) is, however, quite different for surfaces *A* and *C* and for surface *A* at different angles of incidence. In the near field ($x_3 \leq \lambda$) $C(x_1, x_3; x_1', x_3|\omega)$ oscillates with a single period, while the amplitude of these oscillations depends, of course, on the parameters δ and a characterizing the surface roughness. These oscillations are due to the excitation of surface plas-

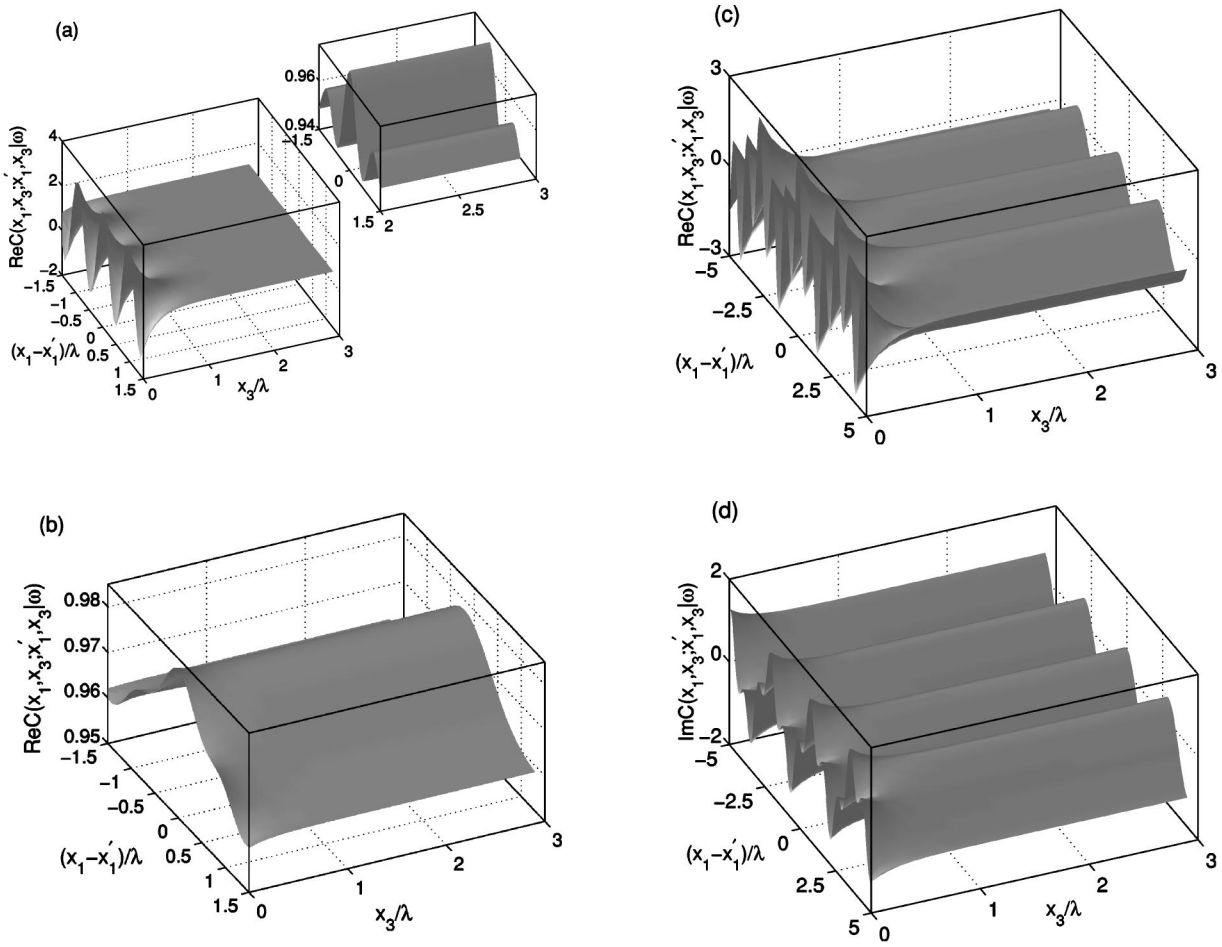

FIG. 2. The real part of the correlation function $C(x_1,x_3;x_1',x_3|\omega)$ as a function of $(x_1-x_1')/\lambda$ and x_3/λ when p-polarized light of wavelength λ is incident normally on (a) surface A and (b) on surface C; and the real (c) and imaginary (d) parts of the correlation function $C(x_1,x_3;x_1',x_3|\omega)$ as a function of $(x_1-x_1')/\lambda$ and x_3/λ when light is incident at an angle $\theta_0=20^\circ$ on surface A.

mon polaritons supported by the rough metallic surfaces, and their period is the surface plasmon polariton wavelength $\lambda_{sp}(\omega)$. Only the contribution $C(x_1,x_3;x_1',x_3|\omega)_{ev}$ to the correlation function displays this type of oscillations. In the case of oblique incidence $C(x_1,x_3;x_1',x_3|\omega)$ displays additional oscillations [see Figs. 2(c) and 2(d)] of a larger period, $\lambda/\sin\theta_0$, which are due to the presence of the factor $\exp[ik(x_1-x_1')]$ in the contribution from the specularly reflected field $|R(k)|^2\exp[ik(x_1-x_1')]$. These oscillations are carried out to the far field also. However, in the far field $C(x_1,x_3;x_1',x_3|\omega)$ as a function of x_1-x_1' oscillates even when light is incident normally on the surface [see, as an example, the inset to Fig. 2(a)]. The period of these oscillations is λ, and they are due to the excitation of lateral waves. Below we discuss in detail the different contributions to the correlation function and the origin of the processes that give rise to the oscillations of the correlation function.

We next turn to a consideration of the dependence of $C(x_1;x_1'|\omega)_{hom}$ on the difference (x_1-x_1'). In Fig. 3(a) we have plotted the real part of this function for the scattering of p-polarized light incident normally on surfaces A, B, and C. For the roughness and experimental parameters assumed in calculating this function the imaginary part of $C(x_1;x_1'|\omega)_{hom}$ is 17 orders of magnitude smaller than the real part, and will not be considered further here. For the two smaller correlation lengths $\mathrm{Re}\,C(x_1;x_1'|\omega)_{hom}$ is an oscillatory function of (x_1-x_1') with a period given by $T_1=\lambda$, the wavelength of the incident light. These oscillations are associated with the branch points of the integrand in Eq. (4.28) at $q=\pm(\omega/c)$, i.e., they are due to the excitation of lateral waves. After the few first oscillations, which are strongly influenced by the central peak in $\mathrm{Re}\,C(x_1;x_1'|\omega)_{hom}$, which has quite a different origin, the amplitude of these oscillations decreases with increasing distance x_1-x_1' algebraically as $|x_1-x_1'|^{-3/2}$. It depends strongly on the correlation length of the surface roughness, as $\exp[-(\pi a/\lambda)^2]$ and, consequently, for a correlation length $a=400$ nm (surface C) is so small that the oscillations are not visible on the scale of this figure. The form of $\mathrm{Re}\,C(x_1;x_1'|\omega)_{hom}$ between the first minima on either side of the maximum at $x_1-x_1'=0$, i.e., for $-\lambda\lesssim(x_1-x_1')\lesssim\lambda$, reflects the surface height autocorrelation function $W(|x_1-x_1'|)$. It is closer to $W(|x_1-x_1'|)$ the larger is the correlation length a. This is easy to understand from an analysis of the integral (4.28). Indeed, for a weakly rough surface the main contribution to the integral comes from the single scattering contribution $X(q|k)$ which contains the power spectrum of the

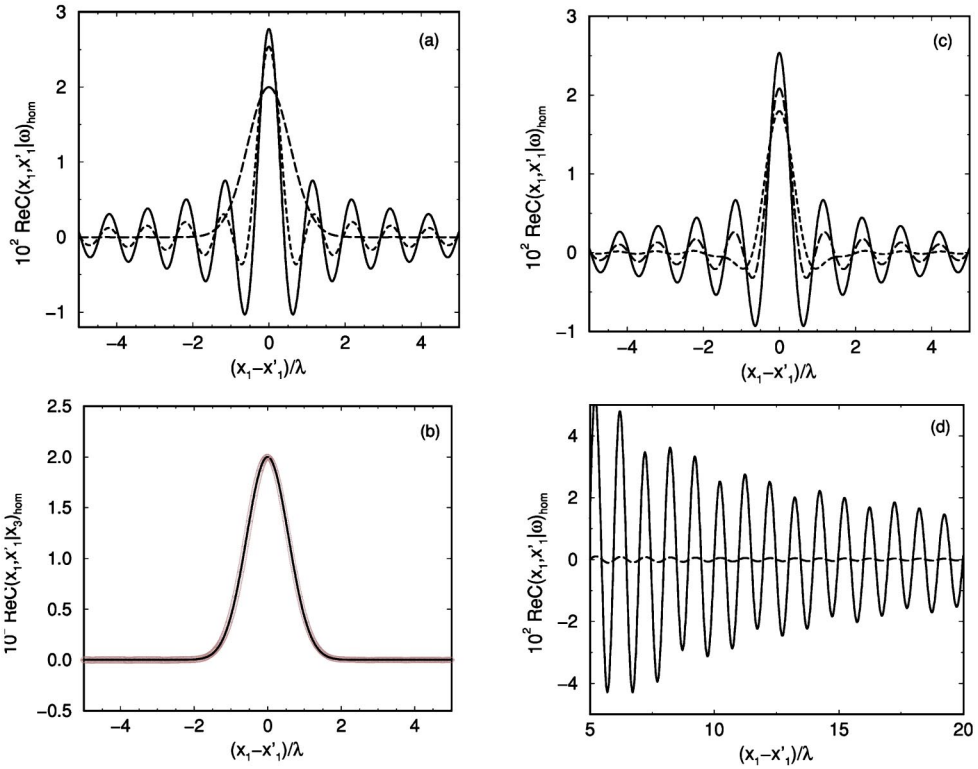

FIG. 3. (a) Re $C(x_1;x_1'|\omega)_{\mathrm{hom}}$ as a function of $(x_1-x_1')/\lambda$ when p-polarized light of wavelength λ is incident normally on surface A(——), surface B(– – – –), and surface C(- - - - -) (b) Re $C(x_1;x_1'|\omega)_{\mathrm{hom}}$ ($\diamond\ \diamond\ \diamond\ \diamond$) as a function of $(x_1-x_1')/\lambda$ when p-polarized light of wavelength λ is incident normally on surface C, together with a plot of $A\exp[-(x_1-x_1')^2/a^2]$ as a function of $(x_1-x_1')/\lambda$, where $a=400$ nm; (c) Re $C(x_1;x_1'|\omega)_{\mathrm{hom}}$ as a function of $(x_1-x_1')/\lambda$ when p-polarized light of wavelength λ is incident at an angle $\theta_0=20^\circ$ on surface A(——), surface B(– – – –), and surface C(- - - - -); (d) Re $C(x_1;x_1'|\omega)_{\mathrm{hom}}$ as a function of $(x_1-x_1')/\lambda$ when p-polarized light of wavelength λ is incident at an angle $\theta_0=20^\circ$ on surface A' (——) and C'(- - - - - -).

surface roughness. The larger the correlation length the narrower the power spectrum. As a result the integrand in Eq. (4.28). becomes a function that is highly peaked around $q=0$. On removing the slowly varying parts of the integrand outside the integral, we find that at normal incidence $C(x_1;x_1'|\omega)_{\mathrm{hom}}$ with quite a high accuracy has the form

$$C(x_1;x_1'|\omega)_{\mathrm{hom}} \approx 16\pi^2\left(\frac{\delta}{\lambda}\right)^2\left|\frac{\sqrt{\epsilon(\omega)}-1}{\sqrt{\epsilon(\omega)}+1}\right|^2 \times\exp\left[-(x_1-x_1')^2/a^2\right]. \tag{5.1}$$

This is illustrated in Fig. 3(b), where we have plotted Re $C(x_1;x_1'|\omega)_{\mathrm{hom}}$ as a function of x_1-x_1' for the same values of the experimental parameters used in obtaining Fig. 3(a), for surface C. Also plotted is the function $0.019\exp[-(x_1-x_1')^2/a^2]$, where the value of the coefficient in front of the Gaussian is estimated from Eq. (5.1). The former curve lies directly on top of the latter. For smaller correlation lengths the contribution to $C(x_1;x_1'|\omega)_{\mathrm{hom}}$ given by Eq. (5.1) is also dominant for small values of $|x_1-x_1'|\lesssim\lambda$, but becomes distorted by the contribution from the lateral waves.

When the angle of incidence is increased from $\theta_0=0°$ to $\theta_0=20°$, with all the roughness and remaining experimental parameters retaining the values used in obtaining Fig. 3(a), the resulting function Re $C(x_1;x_1'|\omega)_{\mathrm{hom}}$ plotted against (x_1-x_1') is presented in Fig. 3(c). In this case the oscillations of this function have two periods: a period $T_1=\lambda$ arising from the branch points at $q=\pm\omega/c$ of the integrand in Eq. (4.28), and a larger period $T_2=\lambda/\sin\theta_0$ arising from the poles of the integrand in Eq. (4.28) at $q=-k\pm i2\Gamma$. The latter oscillations have considerably smaller amplitude than the former, because they are due to multiple scattering processes. Their amplitude can be estimated from Eq. (4.28), and is

$$\begin{aligned}&\approx 2\pi a^2\delta^4\cos^2\theta_0\frac{\omega^2}{c^2}\frac{C^2(\omega)}{\Gamma}\left|\frac{\epsilon(\omega)-1}{\epsilon^2(\omega)}\right|^4|G(k)|^4\\&\times\left\{2\Delta(\omega)|\epsilon|^2\frac{\omega^2}{c^2}|k_{\mathrm{sp}}^2-k^2|\exp[-(k-k_{\mathrm{sp}})^2a^2/4]\right.\\&\times\exp[-(k+k_{\mathrm{sp}})^2a^2/4]+\Delta_{\mathrm{sp}}(\omega)|\epsilon k_{\mathrm{sp}}k+\alpha(k)\alpha(k_{\mathrm{sp}})|^4\\&\times\exp[-(k+k_{\mathrm{sp}})^2a^2/2]+\Delta_{\mathrm{sp}}(\omega)|\epsilon k_{\mathrm{sp}}k-\alpha(k)\alpha(k_{\mathrm{sp}})|^4\\&\left.\times\exp[-(k-k_{\mathrm{sp}})^2a^2/2]\right\}.\end{aligned} \tag{5.2}$$

To demonstrate the presence of the oscillations of the larger period in Fig. 3(d) we present plots of the function Re $C(x_1;x_1'|\omega)_{\mathrm{hom}}$ calculated for the surfaces we denoted A' and C', which are characterized by the same correlation

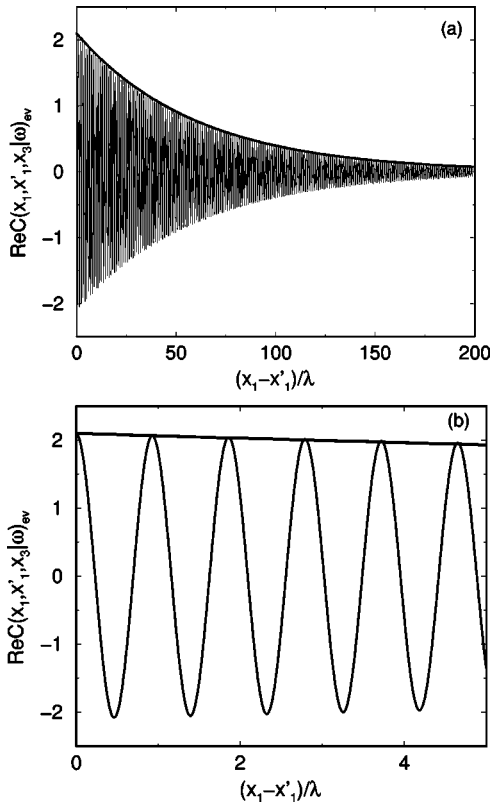

FIG. 4. (a) A plot of $C(x_1,x_3;x_1',x_3|\omega)_{\rm ev}$ as a function of (x_1-x_1') for $x_3=\lambda/10$ when p-polarized light of wavelength λ is incident normally on surface A, together with a plot of $C_{\rm max}\exp[-|x_1-x_1'|/L_{\rm sp}(\omega)]$; (b) an enlargement of (a) in the region of small $(x_1-x_1')/\lambda$.

lengths as the surfaces A and C but by an rms height $\delta=15$ nm.

Finally, we examine the dependence of $C(x_1,x_3;x_1',x_3|\omega)_{\rm ev}$ on (x_1-x_1') at a fixed value of x_3 in the near field. In Fig. 4(a) we plot $\mathrm{Re}\,C(x_1,x_3;x_1',x_3|\omega)_{\rm ev}$ for surface A as a function of x_1-x_1' for a value of $x_3=\lambda/10$. The angle of incidence is $\theta_0=0°$. $\mathrm{Re}\,C(x_1,x_3;x_1',x_3|\omega)_{\rm ev}$ is seen to be a rapidly oscillating function of (x_1-x_1'). The period of these oscillations is $\lambda_{\rm sp}(\omega)=2\pi/k_{\rm sp}(\omega)$, as can be seen from Fig. 4(b), and they arise from the poles of $G(q)$ at $q=\pm[k_{\rm sp}(\omega)+i\Delta(\omega)]$ in the integrand of Eq. (4.29), i.e., they arise due to the excitation of surface plasmon polaritons. Keeping in mind that the dominant contribution to the integral in Eq. (4.29) comes from the first term in its integrand, namely the contribution from single scattering processes, the pole contribution to it can be easily estimated with the result that at normal incidence we obtain

$$C(x_1,x_3;x_1',x_3|\omega)_{\rm ev}\approx 8\pi\sqrt{\pi}a\delta^2\frac{\omega^3}{c^3}\frac{|\epsilon_1(\omega)|^{3/2}}{[\epsilon_1(\omega)+1]^2}\times\exp[-k_{\rm sp}^2a^2/4]\cos[k_{\rm sp}(x_1-x_1')]\times\exp[-2\Delta(\omega)|x_1-x_1'|]\times\exp[-2x_3(\omega/c)\mathrm{Re}(1/\sqrt{-\epsilon(\omega)-1})]. \quad (5.3)$$

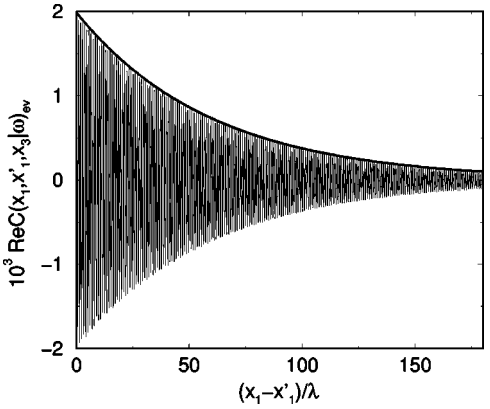

FIG. 5. The same as Fig. 4 but for surface C.

Thus these oscillations have an exponentially decreasing envelope function of the form $C_{\rm max}\exp[-|x_1-x_1'|/L_{\rm sp}(\omega)]$, where $L_{\rm sp}(\omega)$ is the energy mean free path of the surface plasmon polariton of frequency ω supported by the randomly rough vacuum-metal interface. It is given by $L_{\rm sp}(\omega)=[2\Delta(\omega)]^{-1}$, and in the present case has the value $L_{\rm sp}(\omega)=62.2\lambda$. When the transverse correlation length of the surface roughness is increased to $a=400$ nm (surface C), with the remaining roughness and experimental parameters retaining the values used in obtaining Figs. 4, $\mathrm{Re}\,C(x_1,x_3;x_1',x_3|\omega)_{\rm ev}$ has the same oscillatory dependence on (x_1-x_1') as it does when $a=100$ nm, with the same period $\lambda_{\rm sp}(\omega)$ and an exponentially decreasing envelope function with the same decay length $L_{\rm sp}(\omega)$ (Fig. 5). The only significant effect of the fourfold increase in the value of a is that the amplitude of the exponentially decreasing envelope of the oscillations, $C_{\rm max}$, is reduced by a factor of 10^3. This is because for the value of $k_{\rm sp}(\omega)$ arising from the values of λ and $\epsilon(\omega)$ assumed in the present work, a fourfold increase in a produces a three orders of magnitude decrease in the power spectrum of the surface roughness $\sqrt{\pi}a\exp[-k_{\rm sp}^2(\omega)a^2/4]$, which means that the efficiency of the excitation of surface plasmon polaritons is three orders of magnitude weaker for the surface C than for the surface A.

VI. CONCLUSIONS

We can draw several conclusions from the results obtained in this investigation. The first is that the spatial coherence of the electromagnetic field scattered from a one-dimensional randomly rough metal surface measured in the far field, i.e., several wavelengths away from the surface, does not change with distance from the surface. The second is that in the near field the spatial coherence depends significantly on the distance from the surface. Its magnitude depends strongly on the magnitude of the transverse correlation length of the surface roughness a for a fixed value of the rms height of the surface, and decreases as a increases. The third is that the spatial coherence of the electromagnetic field measured in the far field as a function of x_1-x_1' at a fixed distance from the mean scattering surface mimics the surface height autocorrelation function for small values of (x_1-x_1')

and oscillates with two periods, $T_1=\lambda$ and $T_2=\lambda/\sin\theta_0$, where θ_0 is the angle of incidence. The oscillations with the first period arise from the branch points at $q=\pm(\omega/c)$ present in the Green's function $G(q)$ in the integrand in Eq. (4.28), and their amplitude greatly decreases with an increase of the transverse correlation length of the surface roughness. The oscillations with the second period arise from the denominator $(q+k)^2+4\Gamma^2$ in the integrand in Eq. (4.29). The fourth is that the spatial coherence of the electromagnetic field measured in the near field as a function of x_1-x_1' at a fixed distance from the mean scattering surface oscillates with the period $T=\lambda_{sp}(\omega)$, where $\lambda_{sp}(\omega)=2\pi/k_{sp}(\omega)$ is the wavelength of the surface plasmon polaritons supported by the vacuum-metal interface. The exponential decay of the amplitude of these oscillations is characterized by the decay length $L_{sp}(\omega)$, the energy mean free path of the surface plasmon polaritons of frequency ω supported by the randomly rough vacuum-metal interface.

In closing we note that from an experimental standpoint it may be easier to measure the correlation function of the total magnetic field in the vacuum region,

$$\Gamma(x_1,x_3|x_1',x_3'|\omega)=\langle H_2(x_1,x_3|\omega)H_2^*(x_1',x_3'|\omega)\rangle, \quad (6.1)$$

where $H_2(x_1,x_3|\omega)$ is given by Eq. (3.1). The relation between $\Gamma(x_1,x_3;x_1',x_3'|\omega)$ and $C(x_1,x_3;x_1',x_3'|\omega)$ is

$$\Gamma(x_1,x_3;x_1',x_3'|\omega)=C(x_1,x_3;x_1',x_3'|\omega)+\exp[ik(x_1-x_1')-i\alpha_0(k)(x_3-x_3')]+2\exp[ik(x_1-x_1')]\mathrm{Re}\{R(k)\exp[i\alpha_0(k)(x_3+x_3')]\}. \quad (6.2)$$

On setting $x_3=x_3'$ we obtain

$$\Gamma(x_1,x_3;x_1',x_3|\omega)=C(x_1,x_3;x_1',x_3|\omega)+\{1+2\,\mathrm{Re}(R(k)\times\exp[2i\alpha_0(k)x_3])\}\exp[ik(x_1-x_1')]$$
$$=C(x_1,x_3;x_1',x_3|\omega)+\{1+2A(k)\times\cos[2\alpha_0(k)x_3+\phi(k)]\}\times\exp[ik(x_1-x_1')], \quad (6.3)$$

where

$$A(k)=|R(k)|, \quad \tan\phi(k)=\frac{\mathrm{Im}\,R(k)}{\mathrm{Re}\,R(k)}. \quad (6.4)$$

If for a given value of $k=(\omega/c)\sin\theta_0$ we can determine the amplitude $A(k)$ and phase $\phi(k)$ of $R(k)$, then Eq. (6.3) allows us to obtain $C(x_1,x_3;x_1',x_3|\omega)$ from a determination of $\Gamma(x_1,x_3;x_1',x_3|\omega)$ for that value of k. To do this we set $x_1=x_1'$ and obtain

$$\Gamma(x_1,x_3;x_1,x_3|\omega)=C(x_1,x_3;x_1,x_3|\omega)+1+2A(k)\times\cos[2\alpha_0(k)x_3+\phi(k)]. \quad (6.5)$$

A measurement of $\Gamma(x_1,x_3;x_1,x_3|\omega)=\langle|H_2(x_2,x_3|\omega)|^2\rangle$ in the far field $x_3\gg\lambda$, where $C(x_1,x_3;x_1,x_3|\omega)=\langle|H_2(x_2,x_3|\omega)_{sc}|^2\rangle$ is now a constant whose value depends on k, $C(k)$, yields

$$\Gamma(x_1,x_3;x_1,x_3|\omega)=C(k)+1+2A(k)\times\cos[2\alpha_0(k)x_3+\phi(k)], \quad x_3\gg\lambda. \quad (6.6)$$

The oscillations of the intensity of the total magnetic field in the vacuum region as a function of x_3 are just the well known Wiener fringes [19]. From the result given by Eq. (6.6). the values of $A(k)$ and $\phi(k)$ can be determined, and hence $C(x_1,x_3;x_1',x_3|\omega)$ for that value of k.

ACKNOWLEDGMENTS

The research of T.A.L. and A.A.M. was supported in part by U. S. Army Research Office Grant No. DAAD 19-02-1-0256; the research of J.M.-L. was supported by U. S. Office of Naval Research Grant No. N 00014-00-1-0672 and by UC-MEXUS.

[1] W. H. Carter and E. Wolf, J. Opt. Soc. Am. **65**, 1067 (1975).
[2] R. Carminati and J.-J. Greffet, Phys. Rev. Lett. **82**, 1660 (1999).
[3] A. V. Shchegrov, K. Joulain, R. Carminati, and J.-J. Greffet, Phys. Rev. Lett. **85**, 1548 (2000).
[4] T. Setala, M. Kaivola, and A. T. Friberg, Phys. Rev. Lett. **88**, 123902 (2002).
[5] K. P. Gaikovich, A. N. Reznik, V. L. Vaks, and N. V. Yurasova, Phys. Rev. Lett. **88**, 104302 (2002).
[6] H. Roychowdhury and E. Wolf, Opt. Lett. **28**, 170 (2003).
[7] A. Apostol and A. Dogariu, Phys. Rev. E **67**, 055601 (2003).
[8] A. Apostol and A. Dogariu, Phys. Rev. Lett. **91**, 093901 (2003).
[9] E. Wolf and W. H. Carter, Opt. Commun. **50**, 131 (1984).
[10] G. Brown, V. Celli, M. Haller, A. A. Maradudin, and A. Marvin, Phys. Rev. B **31**, 4993 (1985), Appendix A.
[11] A. R. McGurn, A. A. Maradudin, and V. Celli, Phys. Rev. B **31**, 4866 (1985).
[12] Lord Rayleigh, *Theory of Sound* (MacMillan, London, 1895), 2nd ed. Vol. II, pp. 89 and 297.
[13] N. R. Hill and V. Celli, Phys. Rev. B **17**, 2478 (1978).
[14] F. Toigo, A. Marvin, V. Celli, and N. R. Hill, Phys. Rev. B **15**, 5618 (1977).
[15] G. C. Brown, V. Celli, M. Coopersmith, and M. Haller, Surf. Sci. **129**, 507 (1983).
[16] The details of the calculations leading to Eq. (4.20) can be found in Ref. [17].
[17] A. V. Zayats, I. I. Smolyaninov, and A. A. Maradudin, Phys. Rep. **408**, 131 (2005).
[18] P. B. Johnson and R. W. Christy, Phys. Rev. B **6**, 4370 (1972).
[19] M. Born and E. Wolf, *Principles of Optics*, 7th ed. (Cambridge University Press, Cambridge, England, 1999), pp. 311–313.